The concentration factor on the mixture of Ag paste and H₃PO₄ solution as a dopant paste for contact formation in silicon solar cells

The concentration factor on the mixture of Ag paste and H_3PO_4 solution as a dopant paste for contact formation in silicon solar cells

N. A. M. Sinin[a], A. R. M. Rais[a,b], K. Sopian[c], M. A. Ibrahim[a,*]
aSolar Energy Research Institute, Universiti Kebangsaan Malaysia, 43600 Bangi, Selangor, Malaysia
bSchool of Physics, Universiti Sains Malaysia, 11800 Penang, Malaysia
cDepartment of Mechanical Engineering, Universiti Teknologi PETRONAS, 32610, Seri Iskandar, Perak Darul Ridzuan, Malaysia

Screen printing dopant is a new technique to create emitter regions on solar cells. On top of the emitter region, there will be screen-printed metallic contacts that are commonly used silver as front contact. Both processes are performed in separate procedure which requires two different diffusion process involving a high-temperature process. Silver makes good ohmic contact on both light and heavily doped. A solution is proposed by applying a single step of screen printing and annealing process of Ag and phosphorus acid. Simultaneous annealing of Al, Ag, Ag/P screen-printed pastes form diodes with and without heavily doped phosphorous layers under Ag contacts on n-type and p-type silicon wafers by annealing at a constant temperature of 900℃ while varying annealing time from 10-40 seconds at a 10-second interval. The cross-section image of 5% and 10% of Ag/P was measured by using FESEM with EDX report has identified the presence of phosphorus in the Ag/P paste. Dark IV shows an ohmic contact for both p- and n-type. The ability to form the Ag/P paste in the screen-printing process makes it amenable to use as a self-dopant paste process in solar cells.

1. Introduction

One of the crucial phases in the production of solar cells is the development of contacts. For high-efficiency screen-printed solar cells, good front contact formation is essential. The shadowing and series resistance losses, as well as the emitter diffusion profile and surface doping concentration, are all determined by the metallization process used [1][2]. For contact metallization, photolithography and buried-contact procedures are time-consuming and costly. Because of its cost-effectiveness, speed and ease of production, screen printing is commonly employed in industrial metallization [3]. Furthermore, the metallization technology is extremely adaptable, and it may be used with a variety of materials for PV applications, including etch resist, etching paste [4][5], and dopant pastes [6].

The production of commercially viable solar cells based on crystalline Si requires the fabrication of ohmic contacts with contact resistivity below 0.01 Ωcm^2 [7]. Surface dopant concentrations are often required to achieve low contact resistivity in both n-type and p-type Si. The diffusion of dopant atoms into the solar cell at high temperatures produces a highly doped surface. Self-doping contacts, on the other hand, have recently been examined as a possibility to eliminate this separate diffusion step. In this method, and n-type or p-type doping elements are added into the contact such as Aluminum (Al) or Boron (B) for p-type contacts and antimony (Sb) or phosphorus (P) for n-type contacts. The added contact may then be annealed, resulting in a high concentration of the appropriate dopant in the Si surface region, which would improve the ohmic

---

behavior. The predominant industrial technique to establish ohmic contact to an n-type emitter of a crystalline silicon solar cell is screen printing the front grid using a silver-based thick-fil paste [8].

In silicon solar cell fabrication, the contacts are typically applied by screen printing a paste comprising particles of the contact material, then firing or alloying these metals in a belt furnace [9]. Although self-doping and accessible in paste form, Al contacts are not easily solderable and need the addition of an Ag to generate a solderable surface. Some reported that Ag as one of the conducting mediums [10][11]. A combination and evaporating a layer of Ag and P resulted in Ag/P interactions. An Ag/p contacts have also been applied as a paste, with P serving as an intrinsic component of the contact system.

Previous study has been reported on the use of Ag paste in conjunction with dopants as a source of dopants. Meier et al [12] has develop a contact system by combining Ag paste with a dopant source (P or B) by using screen printing process for achieving a selective emitter. Porter et al. [7] used a combination of Ag-based paste doped with red phosphorus powder to developed and characterize of self-doping ohmic contacts on n-type Si. In industrial manufacturing, liquid-source based phosphorus oxychloride (POCl$_3$), as phosphorus gas source in high temperature is widely used for n-type emitter. Unfortunately, the use of POCl$_3$ leads as harmful environment [4]. Therefore, phosphoric acid (H$_3$PO$_4$) is an alternative source dopant which well-known less toxic and environmentally friendly. Alex et al [8] has evaluated different phosphorus sources at level between 0.5% to 3.5% in the Ag paste on different wafers versus a control paste without substantial amount of phosphorus. The result shows that the efficiency of the cell increase from 0.1% to 0.3% on mono-crystalline and poly-crystalline at low levels of phosphorus source. It shows that, better particle dispersion is seen when the phosphorus source is present.

The improvement in the front-side emitter is currently an important issue for the optimization of the silicon solar cell technology [13]. In the present study, we focus on the Ag/P dopant paste as an alternative to a single metallic dopant paste for silicon solar cell to create metallic contact and emitter region on the Si wafer simultaneously. This process is known as the in-situ process of screen-printing silver (Ag) paste with phosphorous (P) dopant from H$_3$PO$_4$, which both are diffused simultaneously. Fig. 1 shows the conventional structure with the aim of this alternative dopant paste structure in Si solar cells This combination can help to reduce several steps of diffusion process in silicon solar cell fabrication. The dark current-voltage characteristics for P-doped contacts are compared to undoped contacts and measured as a function of annealing temperature. Scanning electron microscopy images with energy dispersive X-ray (EDX) analyses provide the present elements in the contacts.
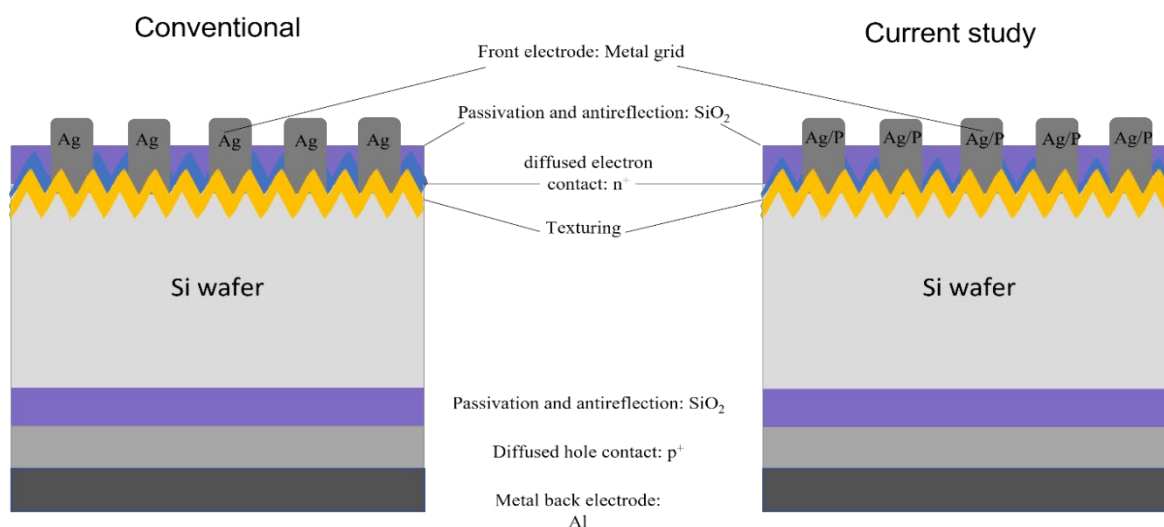

Fig. 1. Comparison Si solar cell structure of conventional and current work.

2. Methodology

Several p-type and n-type single crystalline of (100) orientation was used. The samples were ±175 µm thick and had a resistivity of 0.5~3.0 Ω cm and 10~20 Ω cm respectively. The Si was cleaned by using a mixture of 10% NaOH for 10 minutes and rinsed with deionized water. Then, dipped in HF:H_2O solution with a ratio 1:50 for 1 minutes and rinsed with deionized water to get a hydrophobic surface. Ag-based paste manufactured by Heraeus Materials Singapore PTE LTD was used for the circular contacts to the Si substrates. Fig. 2 shows the overall steps of the process and composition sampling on n-type and p-type Si wafers.
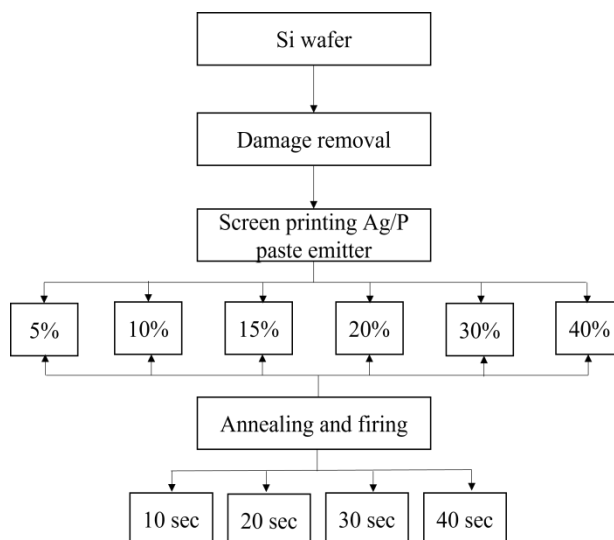
Fig. 2. Process flowchart and different concentration sampling on n-type and p-type Si wafer.

Formation of Ag/P is a combination of silver paste and phosphoric acid as shown in Fig. 3. Silver paste with weighed of 10 mg is mixed with variation of percentage phosphoric acid solution as dopant source. The mixture is swirled constantly for 5 min to make sure it well mixed. The experiment is divided into two parts, formation of an ohmic contact on n-type silicon wafer meanwhile Ag/P formation on p-type wafer silicon shall analyses the diode characteristic. For formation of an ohmic contact, the n-type sample was printed with Ag/P paste with different concentration on both sides as shown in Fig. 4. The samples were subsequently annealed by using 4-inch Quartz Tube Furnace (QTF) instead of conveyor belt Rapid Thermal Annealing (RTA).
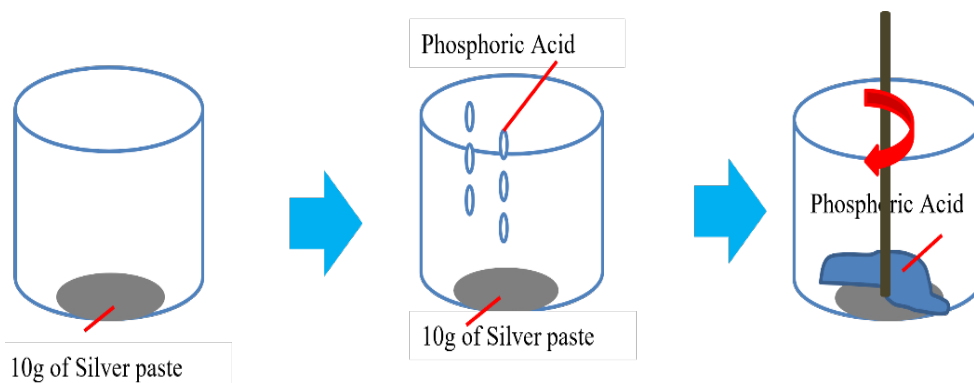

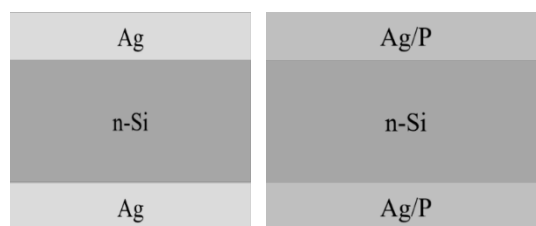*Fig. 3. Method of Ag/P formation by mixing silver paste and phosphoric acid.*

Fig. 4. Ohmic contact structure for n-type for baseline (left) and dopant paste (right).

QTF is a tube furnace with 4-inch diameter, temperature range between 25 to 1100°C is normally used for diffusion process [14]. In this study, the QTF was used for metallization. To avoid wafer bowing, shunting on the junction and over burn on both Ag and Al paste, several optimizations have been done by varying the time holding inside the furnace including the time for inserting and removing the sample. Fast moving in inserting the sample can result ununiformed firing for Al paste meanwhile longer holding time inside the furnace may causes over burn and ripped off from the silicon surface. From the optimization, the samples were annealed at 900°C with 45s for inserting and 45s removing the sample with holding time of 10, 20, 30 and 40s. After annealing process, ohmic behaviour was conducted. Baseline sample in this experiment was prepared using screen printed Ag-based paste on both sides.

Second experiment was carried out to analyse diode characteristic on p-type silicon wafer. Cleaned p-type wafers are screen printed with Ag/P paste on front side whilst Al paste on back side as shown in Fig. 5. The samples were subsequently annealed at 900°C by using quartz tube furnace with 45s in and 45s out with holding time of 10, 20, 30 and 40s. After annealing process, diode behaviour was conducted. Reference sample (Ag) for this experiment was prepared by screen printed Ag-based paste on front side and Al-based paste on back side.
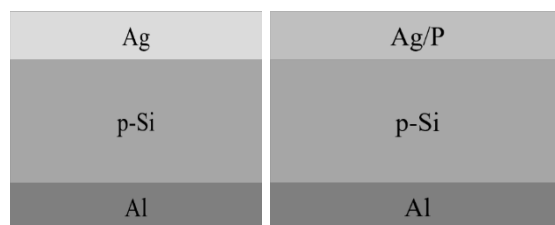

Fig. 5. Diode structure on p-type for baseline (left) and dopant paste (right).

The measurements of the dark current-voltage (I-V) were performed to find the ohmic and diode characteristic. A FESEM with EDX detection system was used for imaging and elemental analysis of the contacts. An ohmic contact was measured by using Dark I-V measurement. Dark I-V response determine an electrical performance of solar cell without the presence of light illumination [15]. Dark I-V measurement carries information about series resistance, shunt resistance and diode factors. In this experiment, series resistance and shunt resistance were calculated by dividing the dark I-V graph into two regions as shown in Fig. 6. The graph was divided and plot again separately to measure the shunt and series resistance by using Linear Squares Fit in Microsoft Excel. After plotting the graph separately, the slope equation was added into the graph. The calculation for shunt and resistance were determined by using equation below:

$$y = mx + c \qquad (1)$$

where m is slope (conductance), and c is the current.

$$slope = \frac{current\ (I)}{voltage\ (V)} \qquad (2)$$

According to Ohm Law equation,

$$Voltage = \frac{Current}{Resistance} \qquad (3)$$

Therefore,

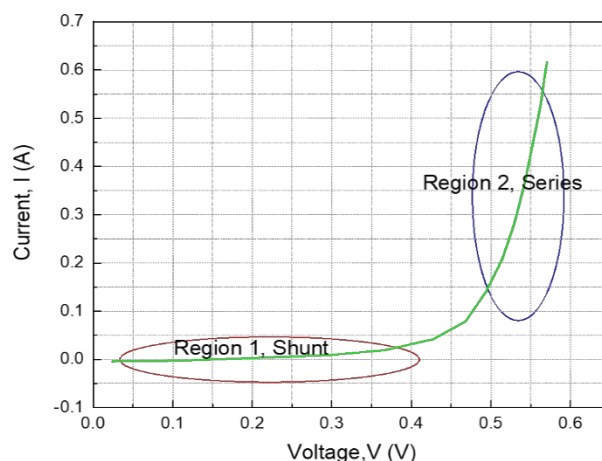$$Resistance = \frac{1}{m} \qquad (4)$$

Fig. 6. Plot of Dark I-V graph on the shunt and series resistance measurement.

3. Results and discussion

The minimum energy needed to move an electron from its bound state into a free state, where it can engage in conduction, is known as the band gap of a semiconductor. Valence band (E_v), the lower energy level of a semiconductor, and conduction band (E_c), the highest energy level at which an electron can be regarded as free.
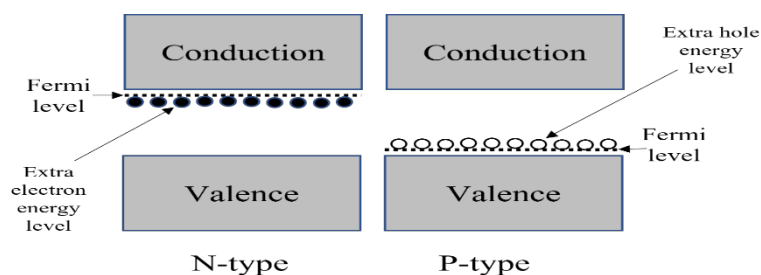
Fig. 7. Energy bands for extrinsic (doped) semiconductor.

The application of band theory to n-type and p-type semiconductors as shown in Fig. 7 shows that extra levels have been added by the impurities. Electron energy levels in n-type materials are close to the top of the band gap, making it simple to excite them into the conduction band. With the energy from an applied voltage, electrons can be propelled to the conduction band and travel through the substance. Extra holes in the band gap for p-type materials enable the excitation of valence band electrons, leaving moving holes in the valence band. With the energy from an applied voltage, electrons can be lifted from the valence band to the holes in the band gap. The holes are referred to as movable because electrons can move back and forth between them.

In this experiment, phosphorus-doped Ag based is the combination of Ag and P materials has been screen printed on both p-type and n-type wafer. Then, the samples were dried in air at 150°C for 15 min. Table 1 shows the topology view result for n and p-type with different Ag/P concentration after drying process. The table shows a different surface texture for each Ag/P concentration. For 5% and 10% of Ag/P, the pastes were completely dry within 15 mins and the texture of pastes are similar with Ag-based after drying proses. However, for 15, 20, 30 and 40% of Ag/P shows a different texture of paste after the drying process. The pastes are not completely dried after 15 mins. The pastes are still wet with similar texture during the screen printing. Due to this condition, the drying process was extended to 45 min, but the result remain the same. Therefore, the experiment was continued by selecting 5% and 10% concentration of Ag/P due to its texture of paste as well as the ease of printing process.

Table 1. Summary of topology view result of different Ag/P concentrations on p-type and n-type Si wafer.
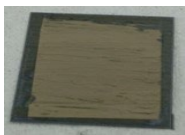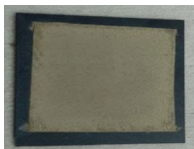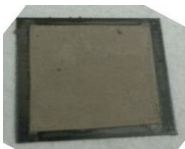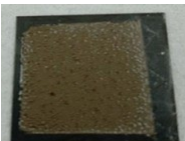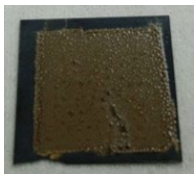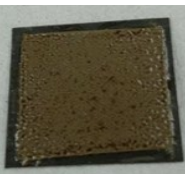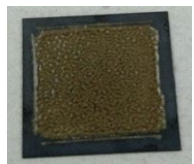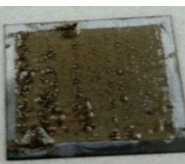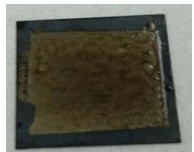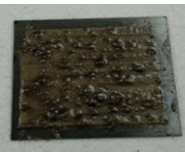
P Concentration	p-type Si Wafer	n-type Si Wafer
5%		
10%		
15%		
20%		
30%		
40%		

Fig. 8 and 9 shows the topology view and cross section images from FESEM for reference (Ag-based) sample and Ag/P (5% and 10%) on n-type and p-type Si wafer for 10s and 40s, respectively. From topology view images, it shows that the adjoining particles fuse together and agglomerate into bunches for reference sample, as well as for n-type and p-type sample with 5%

and 10% concentration for 10s and 40s. For sample with Ag/P concentration, as holding time for annealing increase, the Ag particles agglomerate and left a space between each bunch. Here, the H_3PO_4 solution that contain in the paste take over the space by filling up all the space and create a junction as emitter on the layer of silicon as shown in Fig. 9.
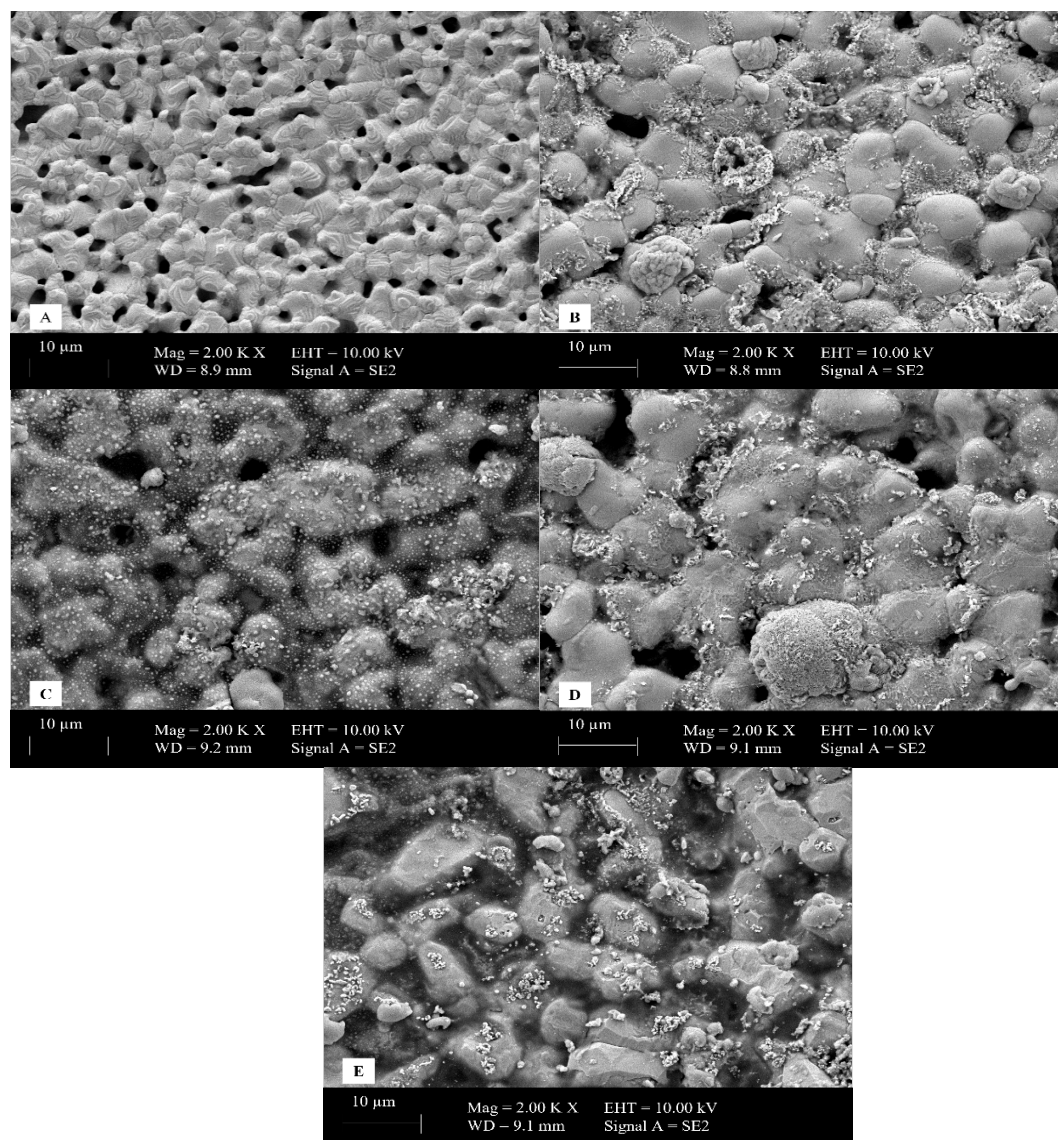

Fig. 8. FESEM top view image of (A) reference (Ag-based paste), (B) 5% of Ag/P for 10s annealing on n-type, (C) 5% of Ag/P for 40s annealing on n-type, (D) 10% of Ag/P for 10s annealing on p-type and (E) 10% of Ag/P for 40s annealing on p-type.

Fig. 9 shows the cross section for reference, n-type, and p-type for each Ag/P concentration (5 and 10%) for 10s and 40s annealing time. As the annealing time increase, the thickness of the paste reduces because of the Ag/P paste diffused and close to silicon surface. Based on the figure, it clearly shows that Ag/P paste diffuse in both type of silicon wafer after firing process and the H_3PO_4 filled up the space between the bunches. This is proved that emitter and contacts layer was formed.
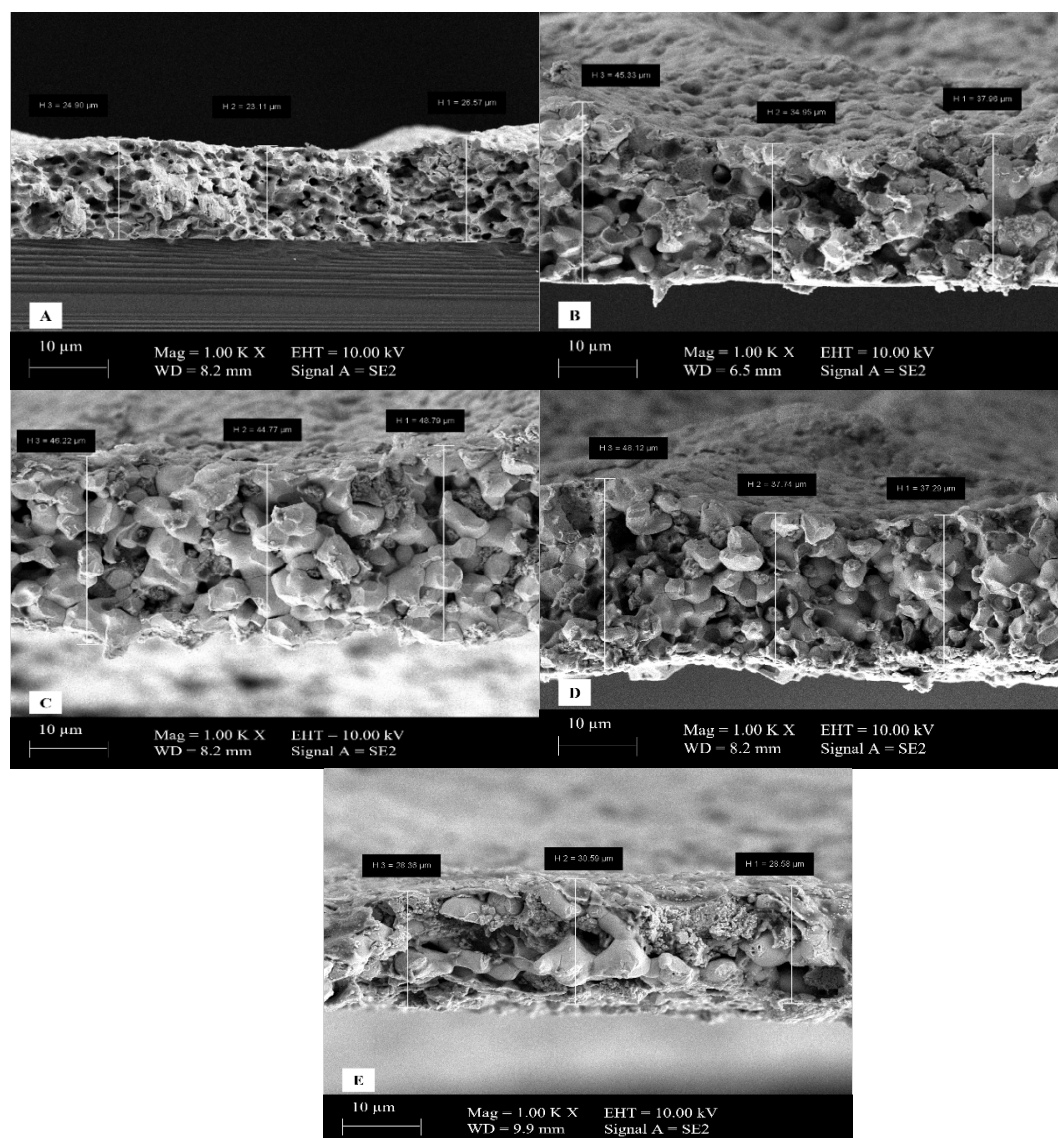
Fig. 9. The cross-section images of (A) reference (Ag-based paste), (B) 5% of Ag/P for 10s annealing on n-type, (C) 5% of Ag/P for 40s annealing on n-type, (D) 10% of Ag/P for 10s annealing on p-type and (E) 10% of Ag/P for 40s annealing on p-type.

Fig. 10 indicate the Energy Dispersion X-ray profile of materials formed on n-type and p-type Si wafer after 5% and 10% Ag/P was annealed at 900 °C for 10s and 40s by using QTF. The EDX mapping has shown the present of Ag on reference sample and both Ag and P element on the Si wafers with Ag/P dopant paste. The diffused phosphorus indicated as the n^+ layer and Ag as contact layer. This figure has confirmed that the formation of Ag/P by combining the Ag-based paste with phosphorus has successfully created.
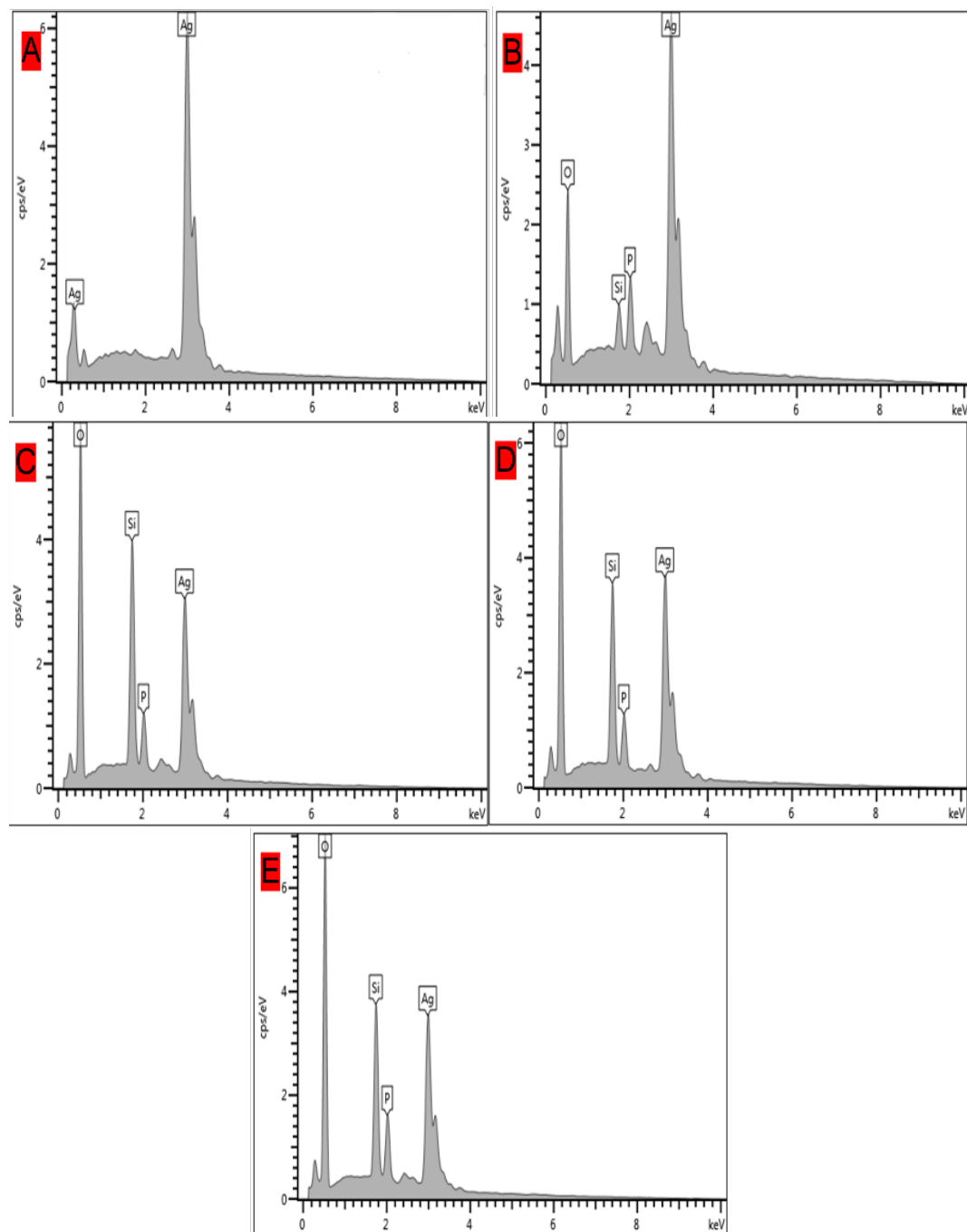
Fig. 10. An EDX report of (A) reference (Ag-based paste), (B) 5% of Ag/P for 10s annealing on n-type, (C) 5% of Ag/P for 40s annealing on n-type, (D) 10% of Ag/P for 10s annealing on p-type and (E) 10% of Ag/P for 40s annealing on p-type.

Fig. 11 represents the dark I-V evaluation of Ag-based paste on n-type Si with different annealing time. Ohmic behaviour for metallization contact of Ag paste and Ag paste doped with pure phosphoric acid is evaluated. Ohmic behaviour is attributed to the corporation of metal-semiconductor interfaces that collects charge carrier across the n-Si and p-Si that will determine the electrical resistance between interfaces [16]. Based on the graph, 10s, 20s, 30s and 40s show an onset of semi-ohmic behaviour after annealing at 900°C for all variations of holding time. The semi-ohmic behaviour for this is due to no P presented with the metallic paste. The low shunt resistance causes power losses in n-Si wafer due to manufacturing and fabrication defects by providing an alternate current path for the light-generated current [17]. Meanwhile, high series

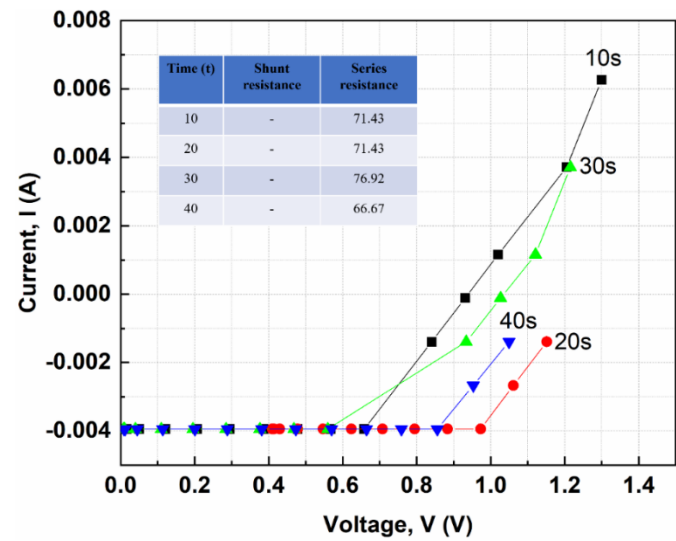resistance calculated from the graph shows that there are movement of current through the emitter and base.

Fig. 11. Dark I-V evaluation of reference (Ag-based paste) on n-type Si with different annealing time.

Fig. 12 presents the dark I-V evaluation for 5% of Ag/P paste on n-the type with different annealing time. From the figure, a semi-ohmic behaviour has been develop for each annealing time. The annealing of 5% Ag/P reveals a substantial reduction in contact resistivity due to the activation of P on the Ag paste. The figure shows an improvement toward ohmic behaviour, which is much better than for Ag-based paste as shown in Fig. 11. Shunt resistance shows inconsistent value due to diode losses its rectifying characteristics. However, the series calculated in the graph confirmed that there are movement of the current through the emitter and base of the n-Si wafer. Thus, the graph shows gave an information that the resistance values show the activation of phosphorus in Ag/P paste on n-type Si. The presence of H_3PO_4 as a P dopant on Ag paste contributes to highly doped on n-Si wafers.
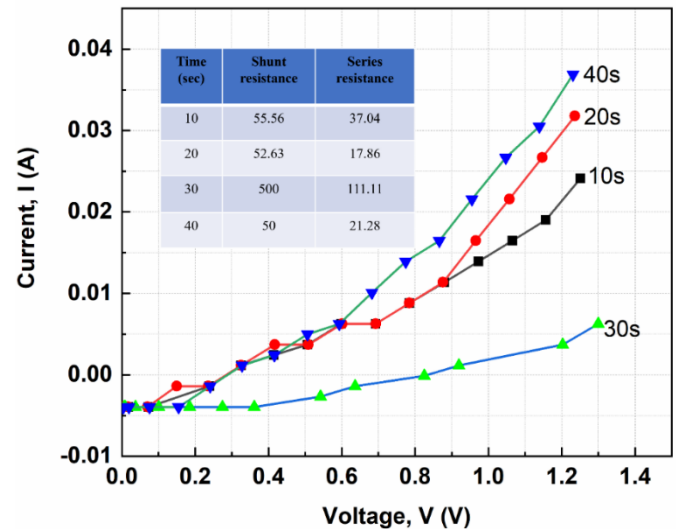

Fig. 12. Dark I-V evaluation for 5% of Ag/P paste on n-type Si with different annealing time.

Fig. 13 represents the dark I-V evaluation for 10% of Ag/P paste on n-type Si with different annealing time. For 10s, 20s and 30s, no ohmic behaviour was detected. While annealing time at 40sec shows an ohmic behaviour. The series resistance and shunt resistance are 6.54 Ω and 10.75 Ω, respectively. The series resistance calculated confirmed that there are movement of the current through the emitter and base. Low shunt resistance gives an impact on power losses due to some defects in manufacturing and fabrication process by providing an alternative current path for light-generated current [18]. Annealing time at 40 sec shows the activation phosphorus in 10% of Ag/P paste on n-type Si. Improvement of semi-ohmic to ohmic behaviour for doped Ag/P paste is associated with an enhancement of P concentration diffused into Si via the co-annealing process. Other than that, is due to well annealed together for both Ag and P in 10% Ag/P paste in in-situ process on the n-Si wafer that makes them accumulate to each other. Ag annealed with P increase the donor (n-type) concentration in the Si wafer. This process of Ag/P was conducted for self-doped of P-doped with Ag with a different type of P and showed promising results on contact resistivity and conductivity [7], [12].
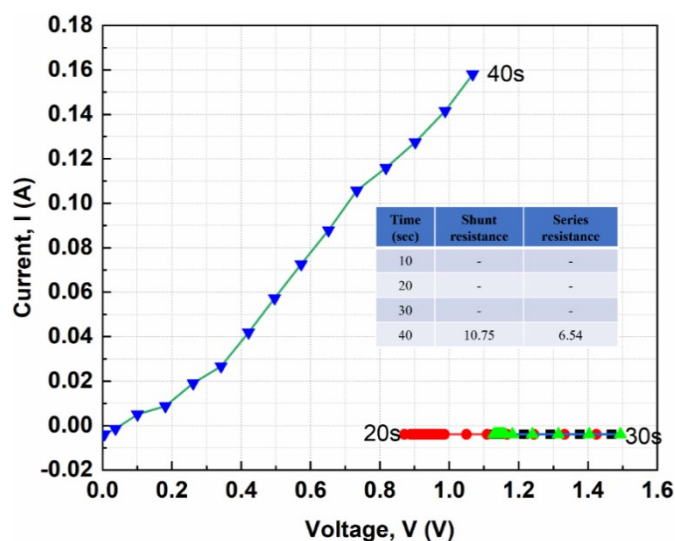

Fig. 13. Dark I-V evaluation for 10% of Ag/P paste on n-type Si with different annealing time.

Fig. 14 shows the dark I-V evaluation of Ag-based paste on p-type Si with different annealing time. Shunt resistance for each different annealing time shows lower value that causes power losses which will create an alternate current path for the light-generated current. thus, reduces the amount of current flowing through the junction and reduces the voltage. While series resistance value calculated in figure shows that there is movement of current through emitter and base in the p-type Si. Because n-Si wafers have greater benefits than p-Si wafers, it is commonly known that n-Si is more tolerant of common defects. This is due to poor minority carrier recombination in n-Si, as the electron easily capture cross section of most impurities is stronger than the hole capture cross section [19], because the electron section is located very close to the conduction band, requiring no or little energy to make the transition.
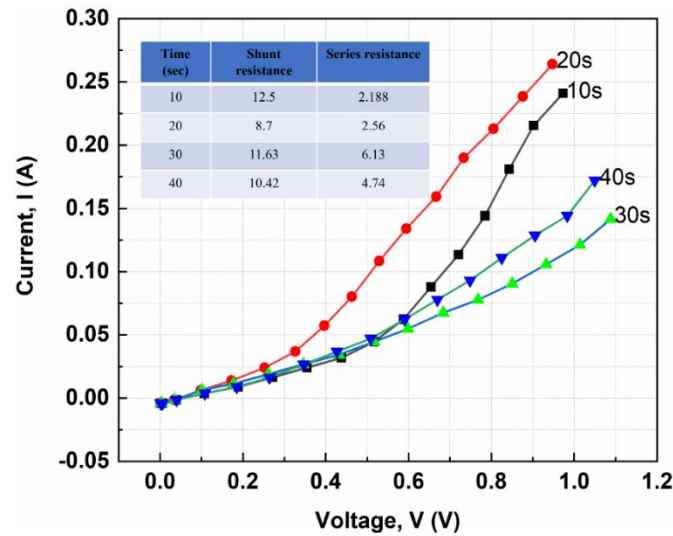
Fig. 14. Dark I-V evaluation of Ag-based paste on p-type Si with different annealing time.

Dark I-V evaluation for 5% of Ag/P paste on p-type Si with different annealing time was presents in Fig. 15. Annealing time for 10s and 20s shows low shunt resistance that cause power losses by providing an alternate current path for light-generated current. for annealing time at 30s and 40s, the value of shunt was below 0 shows a leaky diode with high series resistance. The series resistance calculated for 10s and 20s are 6.54 Ω and 5.92 Ω, respectively. Lower series resistance shows that the Ag/P paste are completely diffused in p-type Si layer and not cause spike of Ag across the emitter region to form contact with the p-type Si. Thus, confirmed that there are movement of the current through emitter and base.
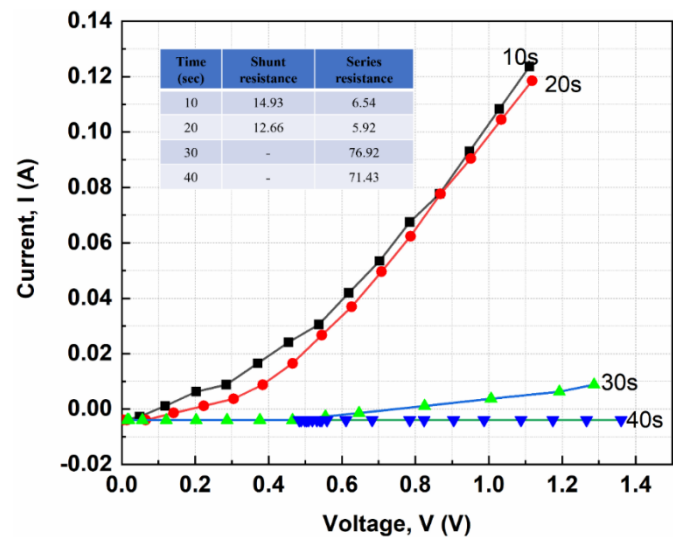

Fig. 15. Dark I-V evaluation for 5% of Ag/P paste on p-type Si with different annealing time.

Figure 16 show a dark I-V evaluation for 10% of Ag/P paste on p-type Si with different annealing time. Annealing time at 20 sec shows highest value for shunt resistance. It indicated lower chances of power losses that will not create an alternative current path for light-generated current. However, for 10 sec and 40 sec shows low shunt resistance that cause impact on power losses by providing an alternate current path for light-generated current caused by some defects in

manufacturing and fabrication process. These resistance value shows an activation of P element in Ag/P paste as an emitter in p-type Si.
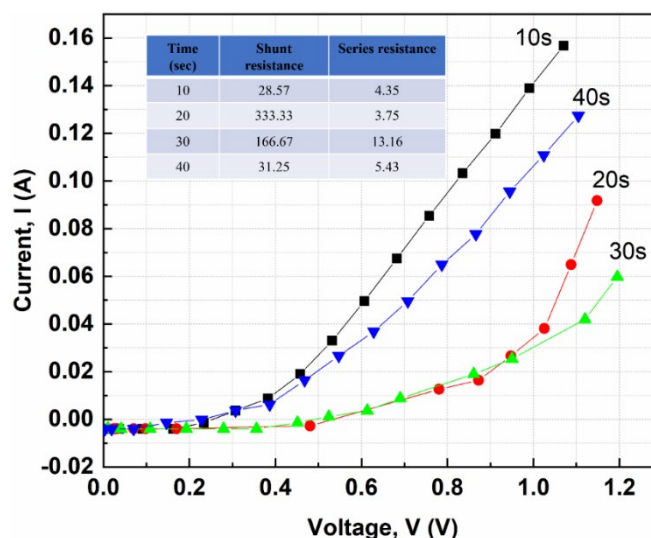

Fig. 16. Dark I-V evaluation for 10% of Ag/P paste on p-type Si with different annealing time.

4. Conclusion

Formation of Ag/P paste with different concentration (5% and 10%) at different time displayed ohmic behaviour on n-type and diode characteristic on p-type Si. The ability to form the Ag/P paste in screen printing process makes it amenable to use as self-dopant paste process in solar cell. Since that, the Ag/P paste with different concentration and annealing time has been confirmed by using dark I-V evaluation, FESEM and EDX profile. The series resistance confirmed that there are movement of current through emitter and base and the presence of shunt due to power losses caused by some defects during manufacturing and fabrication of the Si wafer. The value of resistance also shows that there is activation of phosphorus in the Ag/P paste. 10% Ag/P paste are the most compromising to be used as dopant paste for both n-type and p-type wafer with different annealing time (40 sec, 20 sec) respectively due to its improvement from semi-ohmic to ohmic behaviour and well annealed together in in-situ process on the Si wafer.

Acknowledgments

References

[1] T. Markvart and L. Castener, Solar Cells: Materials, Manufacture and Operation. 2005.
[2] S. Anizan, C. S. Leong, K. L. Yusri, N. Amin, S. Zaidi, K. Sopian, American Journal of Applied Sciences 8(3), 267 (2011); https://doi.org/10.3844/ajassp.2011.267.270
[3] S. Sepeai, M. Y. Sulaiman, S. H. Zaidi, K. Sopian, 2011 IEEE Regional Symposium Micro and Nanoelectronics, RSM 2011 - Program and Abstract, 364 (2011).

694

[4] Z. F. Mohd Ahir, S. Sepeai, S. H. Zaidi, Jurnal Kejuruteraan SI1 (3), 9 (2018);
https://doi.org/10.17576/jkukm-2018-si1(3)-02

[5] G. Katharina, K. Mathias, E. Raphael, K. Markus, P. Maximilian, E. Jonas, 33rd European PV SOlar Energy Conference, 664 (2017).

[6] G. Scardera, D. Inns, G. Wang, S. Dugan, J. Dee, T. Dang, K. Bendimerad, F. Lemmi, H. Antoniadis, Energy Procedia 77, 271 (2015); https://doi.org/10.1016/j.egypro.2015.07.038

[7] L. M. Porter, A. Teicher, D. L. Meier, Solar Energy Materials and Solar Cells 73(2), 209 (2002); https://doi.org/10.1016/S0927-0248(01)00126-X

[8] A. S. Ionkin, B. M. Fish, Z. R. Li, F. Gao, L. K. Cheng, K. Mikeska, C. Torardi, M. Lewittes, P. VerNooy, S. D. Ittel, L. Liang, R. Getty, D. H. Roach, J. G. Pepin, W. J. Borland, 33th IEEE Photovoltaic Specialists Conference, 3179 (2010).

[9] S. M. Ahmad, C. S. Leong, K. Sopian, S. H. Zaidi, Journal of Electronic Materials 47(3), 2120 (2018); https://doi.org/10.1007/s11664-017-6022-7

[10] M. K. Mat Desa, S. Sapeai, A. W. Azhari, K. Sopian, M. Y. Sulaiman, N. Amin, S. H. Zaidi, Renewable and Sustainable Energy Reviews 60, 1516 (2016);
https://doi.org/10.1016/j.rser.2016.03.004

[11] E. Van Kerschaver, G. Beaucarne, Progress in Photovoltaic: Research and Applications 14(2), 107 (2006); https://doi.org/10.1002/pip.657

[12] D. L. Meier, H. P. Davis, R. A. Garcia, J. A. Jessup, A. F. Carrol, Conference Record of Twenty-Eight IEEE Photovoltaic Specialists Conference, 69 (2000).

[13] R. De Rose, M. Zanuccoli, P. Magnone, M. Frei, E. Sangiorgi, and C. Fiegna, IEEE Journal of Photovoltaics 3(1), 159 (2013); https://doi.org/10.1109/JPHOTOV.2012.2214376

14] N. F. Rostan, S. N. Fa. A. Hamid, Z. F. M. Ahir, M. A. Ibrahim, K. Sopian, S. Sepeai, Silicon 14, 12421 (2022); https://doi.org/10.1007/s12633-022-01950-x

[15] S. H. Zaidi, Crystalline Silicon Solar Cells, Springer Nature, Switzerland, 201 (2021);
https://doi.org/10.1007/978-3-030-73379-7_5

[16] D. K. Schroder, D. L. Meier, IEEE Transactions on Electron Devices 31(5), 637 (1984);
https://doi.org/10.1109/T-ED.1984.21583

[17] O. Breitenstein, J. P. Rakotoniaina, M. H. Al Rifai, M. Werner, Progress in Photovoltaics: Research and Pllications 12(7), 529 (2004);
https://doi.org/10.1002/pip.544

[18] A. D. Dhass, E. Natarajan, and L. Ponnusamy, International Conference on Emerging Trends in Electrical and Energy Management, 382 (2012).

[19] A. R. M. Rais, S. Sepeai, M. K. M. Desa, M. A. Ibrahim, P. J. Ker, S. H. Zaidi, K. Sopian, Journal of Ovonic Research, 17(3), 283 (2021); https://doi.org/10.15251/JOR.2021.173.283